

Development of An Advanced Finite Element Model for A Pedestrian Pelvis

Miwako Ikeda

Shunji Suzuki

Yasuaki Gunji

Yukou Takahashi

Honda R&D Co.,Ltd. Automobile R&D Center

Yasuki Motozawa

Masahito Hitosugi

Dokkyo Medical University School of Medicine

Japan

Paper Number 11-0009

ABSTRACT

Because of a highly complex three-dimensional geometry of the pelvis, a variety of load transmission inside the pelvis exists. Due to the variation in pelvis internal load transmission, some of the previous studies revealed a variety of pelvis fracture patterns to pedestrians.

In order to predict pelvis fractures accurately, human finite element (FE) models have been developed in past studies. However, the biofidelity of these pelvis models has not been evaluated sufficiently in terms of pelvis internal load transmission due to the lack of biomechanical data from the literature. In order to address different load paths within the pelvis when subjected to lateral impact load, a recent experimental study investigated the reaction forces at the anterior (i.e., pubic rami) and posterior (i.e., sacrum) sides separately in acetabulum and iliac impacts.

The aim of this study was to improve the biofidelity of a pelvis model by performing additional validations against the published experimental data.

The pelvis model used in this study was based on the FE pelvis model developed in a previous study. The structure and geometry of the baseline pelvis model were further improved. The geometry of the pubic symphysis was newly created by using CT images, and the articular cartilage was added at the acetabulum and SI joint to better represent overall compliance of the pelvis. The overall width of the pelvis was scaled in order to accurately represent the anthropometry of a mid-sized male.

In addition to the response validations performed in the previous study, the pelvis model was subjected to further validations to confirm enhanced biofidelity. Four force-deflection response corridors from the combinations of the impact locations (acetabulum or

iliac crest) and reaction forces (anterior or posterior) were developed in the current study from the published experimental data for dynamic lateral compression of isolated human pelvises. Material parameters of the cortical and trabecular bones were modified to better match the response corridors. The results of the response comparisons showed that the modified pelvis model is capable of representing different load paths within a human pelvis in various loading configurations.

INTRODUCTION

The analysis of the distribution of AIS 2+ injuries by region and vehicle type from NASS-PCDS (National Automotive Sampling System, Pedestrian Crash Data Study, 1994-1998) showed that in pedestrian accidents, leg injuries are most frequent with sedans, while pelvis injuries are most frequent with SUVs [Kikuchi et al., 2008]. In addition, the distribution of injured body regions in pedestrian serious injuries from Japanese accident statistics shows that the number of head injuries in 2009 was dropped by 38.2% compared with that in 1999, while the number of pelvis injuries was only reduced by 7.7%. This suggests that pelvis protection is one of the important issues in pedestrian protection.

Pelvis fractures are classified into several fracture patterns. Among those, the pubic rami are the most frequently injured region in the pelvis. Edwards et al. [1999] investigated the data containing 316 injured pedestrians obtained from the Major Trauma Outcome Study (MTOS), and showed that 61.5% of pedestrian pelvic fractures were pubic rami fractures, of which 17.5% were associated with acetabulum fracture. Ryan [1971] investigated 387 patients admitted to St. Vincent's Hospital in Australia with pelvic fractures due to traffic accidents, and showed

that 78.8% suffered pubic rami fracture, 23.3% suffered acetabulum fracture, and 20.4% suffered iliac fracture. Teresinski et al. [2001] investigated data from the autopsies of 371 pedestrian victims in road traffic accidents in the Department of Forensic Medicine, Medical Academy in Lubin, and showed that fracture of the upper ramus of the pubic bones was observed in 29.6%.

Due to the complex and highly three-dimensional nature of the geometry of the pelvis, it is crucial to represent both anterior and posterior load paths of the pelvis for predicting pelvis fracture accurately. A pelvis FE model can be an appropriate tool for predicting fracture, because it is capable of representing the precise geometrical characteristics of the pelvis. For this reason, many pelvis FE model have been developed in past studies [Renaudin et al., 1993; Dalstra et al., 1995; Plummer et al., 1996; Konosu et al., 2003; Song et al., 2006; Kikuchi et al., 2006; Kikuchi et al., 2008]. However, almost all of these models have only been validated against the experiments conducted by Guillemot et al. [1998], where total reaction forces of the contralateral side of the pelvis were investigated in lateromedial compressive loading into the acetabulum. Since the load distributions of anterior and posterior sides of the pelvis cannot be identified from this experiment, those models needed to be further validated in terms of pelvis internal load distributions.

Salzar et al. [2008] conducted the experiment for the responses of isolated pelvis, where the fixed side of the pelvis was separated such that anterior and posterior loads can be measured individually in acetabulum and iliac crest loadings. Untaroiu et al. [2010] developed a pelvis FE model and validated it against this experiment, however, the model was validated only in acetabulum loadings.

The aim of this study was to improve the biofidelity of a pelvis FE model by means of validating the model against average responses and corridors of anterior and posterior reaction forces in lateromedial compression of the pelvis due to loadings to the acetabulum and the iliac crest.

MODEL DESCRIPTION

In this study, the model development was performed by using PAM-CRASH™ Version 2008.

Geometry

The model used in this study was based on the pelvis FE model developed by Kikuchi et al. [2006]

representing a mid-sized male anthropometry (Figures 1, 2). Since the geometry of the baseline model was created using CT images of the pelvis from a specific human subject that may not be a representative of a mid-sized male, the overall width of the pelvis was scaled to 262 mm taken from the anthropometric data developed by the University of Michigan Transportation Research Institute [Robbins, 1983] to accurately represent the anthropometry of a mid-sized male. Although the pelvis model was geometrically scaled, the thickness of the pelvis cortical bone was kept the same as that of the baseline model because the average thickness of the cortical bone of approximately 0.9 mm used in the baseline model was close to the average thickness of 0.936 mm investigated by Ostertag et al. [2009].

The sacrum was modeled using deformable shell elements, which had been modeled as a rigid body in the baseline model. It was difficult to clearly identify the thickness distribution of the cortical bone of the sacrum from the medical images, and no data for the material property of the sacrum were found in the literature. Therefore, the average thickness of 0.9 mm for the pelvis cortical bone was used for the sacrum. Due to geometrical complexity, the trabecular bone inside the cortical layer was not modeled, and mechanical characteristics were lumped into the cortical layer.

Although the width of the pubic symphysis increases from posterior to anterior [Vix et al. 1971], a uniform width was applied in the baseline model. Therefore, the geometry of the pubic symphysis was modified referring to the CT images taken in the Dokkyo Medical University School of Medicine, University Hospital (Figure 3). The use of the CT images in this study has been approved by the Ethics Committee of the Dokkyo Medical University School of Medicine. The width of the symphysis pubis was set at 5.6 mm and 4.0 mm on the anterior and posterior sides, respectively.

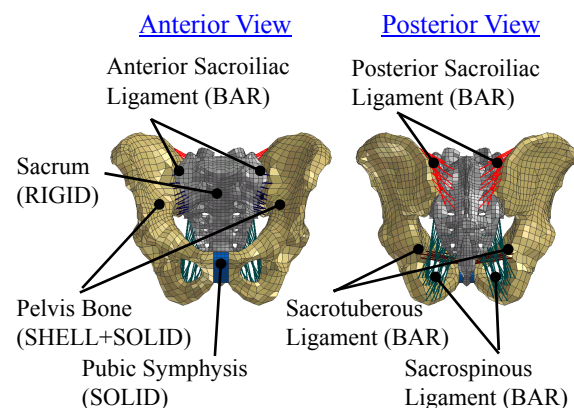


Figure 1. Baseline Pelvis FE Model.

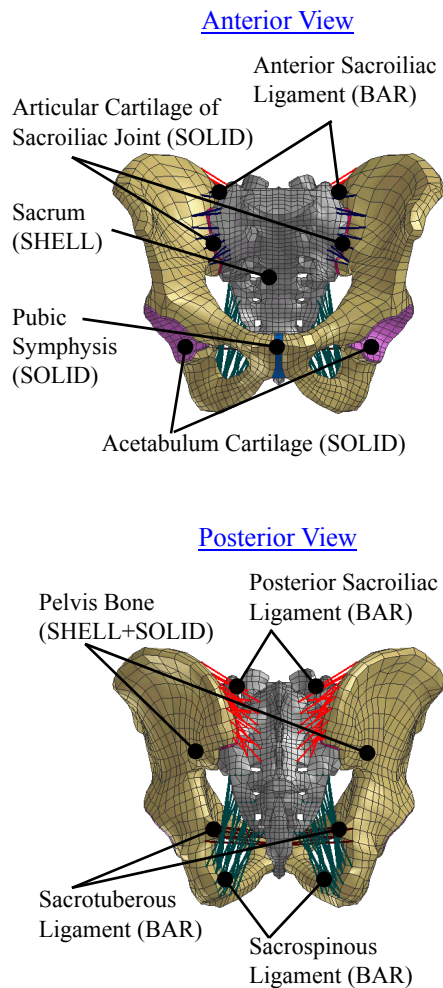


Figure 2. Modified Pelvis FE Model.

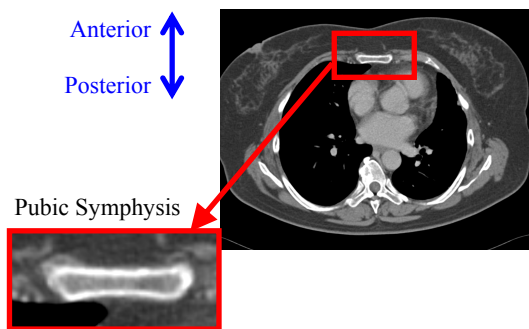


Figure 3. CT Image of Pubic Symphysis.

The articular cartilage represented by solid elements was added to the surfaces of the SI joint and the acetabulum. The thicknesses of the cartilaginous layers at the SI joint and the acetabulum were set at 2.5 mm and 2 mm, respectively, by referring to the anatomical book (Grey's Anatomy [1995]) and the research conducted by Walker [1992] and McLauchlan et al. [2002]. The compressive response of the SI joint was represented by the cartilage

modeled using solid elements, and the tensile response of this joint was represented by the ligaments modeled using tension-only bar elements. The orientations of these ligaments were also modified by referring to the CT images.

Material Property

Pelvis Bone and Sacrum The material parameters of the pelvis bone were tuned based on those of the baseline model so as to match the force-deflection responses of the experiment by Salzar et al. Since the cortical bone is the main component for the stiffness of the pelvis, the parameters chosen in this study were compared to the published data to ensure validity of the tuned parameters. Kemper et al. [2008] conducted tensile tests of the coupon of the cortical bone of the pelvis, and showed that the elastic modulus is 10.9 ± 1.8 GPa, the ultimate stress is 86.4 ± 26.8 MPa, the ultimate strain is 0.016 ± 0.010 . It was found that the parameters chosen in this study (elastic modulus: 9.75 GPa, ultimate stress: 76.9 MPa, ultimate strain: 0.016) were within the range of the experimental data. Because of the lack of data for the sacrum, the same stress-strain curves as those of the pelvis bone were applied, and bone fracture was not simulated, since no complete fracture of the sacrum was seen in the dynamic loadings of the experiment by Salzar et al. Similar to the baseline model, the stress-strain curves of both cortical and trabecular bones were configured so that the strength and stiffness were approximately proportional to the strain rate raised to the 0.06 power referring to the research by Carter et al. [1970]. Bone fracture was represented by using the element elimination option with a total strain criterion except the sacrum. McElhaney et al. [1976] shows the stress-strain curves of human femur in compression in different strain rate (Figure 4). From the figure, the relationship between the ultimate strain and the strain rate was identified for the femur (Equation 1). Due to the lack of data for the pelvis bone, the identical property to that of the femur was applied to the pelvis bone.

$$\epsilon_u = -0.0012 \log_{10} \dot{\epsilon} + \epsilon_{static} \quad (1)$$

ϵ_u : Ultimate Strain, $\dot{\epsilon}$: Strain Rate

ϵ_{static} : Ultimate Strain at $\dot{\epsilon} = 1$

In order to represent the nonlinear stress-strain relationship, strain rate dependency, and the element elimination, MAT143 (elastic-plastic with elastic

stiffening and failure for shell elements) was chosen for the cortical bone and MAT36 (elastic/stiffening-plastic with failure for solid elements) was chosen for the trabecular bone.

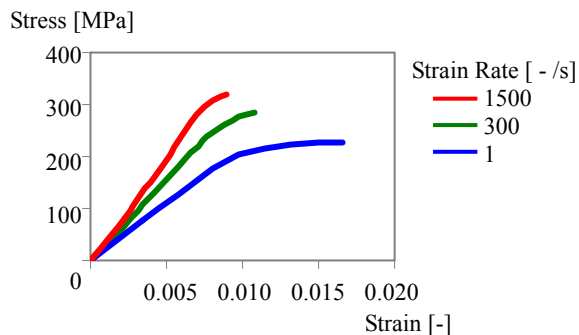


Figure 4. Stress-strain Curves of Human Femur in Compression in Different Strain Rates. [McElhaney et al., 1976].

Pubic Symphysis Due to the lack of information on the material property of the pubic symphysis available from the literature, the material parameters for the pubic symphysis were also tuned during a validation process. Since major loading pattern to the pubic symphysis is compressive loading, the material parameters were determined through the validation against compressive response of the isolated pubic symphysis from the experiment conducted by Dakin et al. [2001]. However, only one compressive response curve was presented in the paper, where the load was applied up to 0.8 mm compression. For this reason, only the initial toe region was determined by validating the model against Dakin et al., and the successive region of the stress-strain curve was determined by validating the model against the force-deflection response of the anterior side of the pelvis in acetabulum impact from the experiment performed by Salzar et al. It was found from these validations that the stiffness of the toe region validated against low speed tests by Dakin et al. was similar to that of the successive region validated against high speed tests by Salzar et al. Therefore, it was decided not to incorporate strain rate dependency. Since complete disruption of the pubic symphysis occurred in only one out of six cases in the dynamic loading to the acetabulum in the experiment performed by Salzar et al., it was decided not to represent failure of the pubic symphysis. In order to represent the nonlinear behavior of the pubic symphysis, MAT36 in PAM-CRASH™ was used and the modulus of the first phase of the material characteristics was set to 1.2 MPa.

Acetabulum Cartilage and Articular Cartilage of Sacroiliac Joint Due to the lack of information available from the literature, the same material property as that of the pubic symphysis was applied to these cartilaginous layers except the stiffer region representing the bottoming. The stiffness of the stiffer region of these layers was determined by validating force-deflection response against the experiment performed by Salzar et al. The strain rate dependency and the rupture were not modeled in the material of these layers. MAT36 in PAM-CRASH™ was chosen for modeling the material of the acetabulum cartilage. As for the articular cartilage of the SI joint, nodes were shared at the interface between the bones (ilium and sacrum) and the cartilage for numerical stability. For this reason, MAT21 in PAM-CRASH™ (elastic foam with hysteresis for solid elements) was chosen in order to provide no tensile resistance from the cartilage.

Sacroiliac Ligaments In order to represent the nonlinear tension-only response of the SI joint, MAT205 (nonlinear tension-only bar element) was chosen for these ligaments. Trilinear stress-strain curve was specified to represent initial toe region as well as less stiff region with high strain. Other ligaments contained in the pelvis model were modeled using the same material models and parameters as those of the baseline model.

AVERAGE RESPONSE AND CORRIDOR FOR PELVIS VALIDATION

Response Curves for Validations

In order to provide validation data for the modified pelvis model, average force-deflection response and corridors were developed based on the test results from Salzar et al. Figure 5 shows the schematics of the test setup. A 76.6 kg drop impactor impacted a transfer beam to which a loading surface to a pelvis specimen was attached. Loads were applied to either the iliac wing or the acetabulum, and load paths through the sacrum and the pubis were separated by cutting the contralateral side of the pelvis to measure posterior (through the sacrum) and anterior (through the pubis) reaction forces individually. As a loading surface, a metallic ball and a padded rigid plate were used for acetabulum and iliac loading tests, respectively. Six dynamic and two quasi-static tests were run for each of the two loading configurations. Due to the limited number of quasi-static tests, the pelvis model was validated against dynamic tests

only. The average impact velocities were 2.8 and 1.9 m/s for the acetabulum and iliac loading tests, respectively. The pubic rami fractured in all of the dynamic acetabulum loading tests. In the dynamic iliac loading tests, two specimens sustained pelvis fracture (at the SI joint and the sacrum) and four subjects sustained laxity or dislocation of the SI joint.

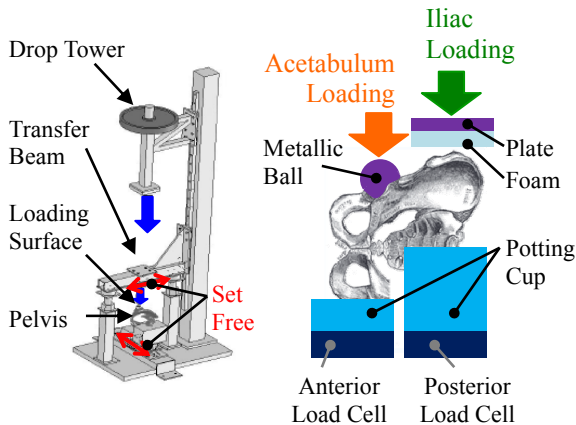


Figure 5. Setup of Experiment Conducted by Salzar et al. [2008].

The average responses and corridors of the anterior or posterior loads in acetabulum and iliac dynamic loadings were developed in this study, using geometrically scaled response curves to average mid-sized male using the standard width of the pelvis (262 mm obtained from the anthropometric data developed by the University of Michigan Transportation Research Institute [Robbins, 1983]). Displacement time histories of the impact surface were calculated by double integrating the acceleration of the transfer beam, and twelve force-deflection curves of the experiment were geometrically scaled in order to represent the response of the mid-sized male.

In the experiment performed by Salzar et al., no direct measurement was done as to the timing of initial contact. For this reason, the force-deflection curves were aligned such that the curves start from certain levels of reaction forces. In case of the acetabulum loading, the force level was set at 100 N for both anterior and posterior reaction forces. In case of iliac loading, 600 N was used for the posterior reaction force because a padded loading surface was used for the iliac loading. The curves for the anterior reaction force were aligned at the timing when posterior reaction force reached 600 N. A video analysis showed that the first peak of the force well correlated with the initiation of pelvis fracture or SI

joint dislocation. Based on this finding, it was decided to interpret the timing of the first peak as the timing of failure, and use the curves up to this timing for response corridor development. Since no peaks were apparent from the anterior reaction force in iliac loading, the timing of failure identified for the posterior reaction force was applied to the anterior reaction force. From the six dynamic iliac loading tests, two of them (#011 and #016) were not used when developing force-deflection corridors because visual inspection showed that the shape of the pelvis was extremely different from others. Figures 6 through 9 show force-deflection curves obtained by following the procedure described above for the four combinations of the loading locations (acetabulum and iliac loadings) and the reaction forces (anterior and posterior reaction forces).

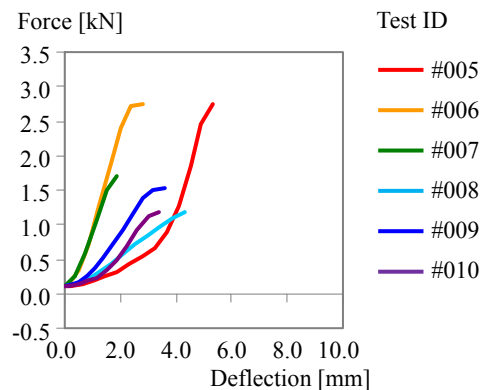


Figure 6. Force-Deflection Response for Anterior Reaction Force in Acetabulum Loading (Scaled to Mid-sized Male).

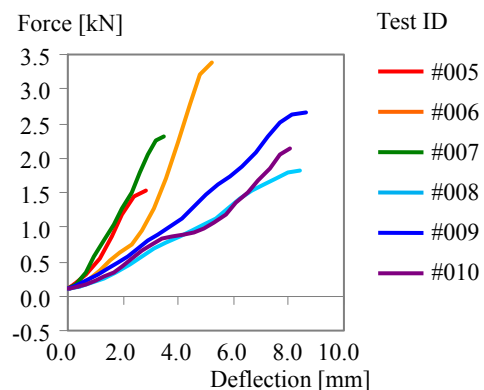


Figure 7. Force-Deflection Response for Posterior Reaction Force in Acetabulum Loading (Scaled to Mid-sized Male).

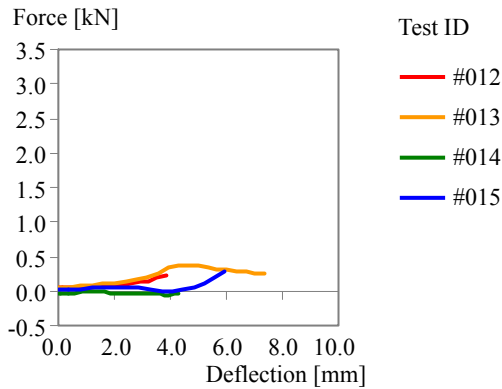


Figure 8. Force-Deflection Response for Anterior Reaction Force in Iliac Loading (Scaled to Mid-sized Male).

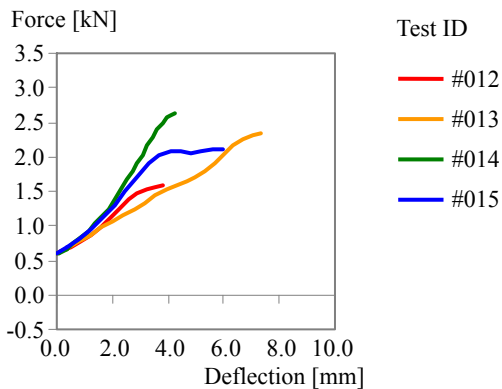


Figure 9. Force-Deflection Response for Posterior Reaction Force in Iliac Loading (Scaled to Mid-sized Male).

Development of Average Response and Corridor

Referring to the scheme for developing corridors proposed by Lessley et al. [2004], the average force-deflection responses and corridors were developed. As an example, the procedure for making them for the anterior reaction force in acetabulum loading is shown below. The same procedure was applied for the posterior reaction force in acetabulum loading and the anterior and posterior reaction forces in iliac loading.

1. For each force-deflection curve, normalize deflection by maximum deflection. (Figure 10)
2. For each force-deflection curve, apply linear interpolation to obtain force values for all normalized curves at every 2 % of the normalized maximum deflection (1.0). (Figure 11)
3. Calculate average and standard deviation of the force values at every 2% of the normalized

maximum deflection to obtain an average curve and upper and lower bounds (average \pm one standard deviation (S.D.)) for normalized deflection. (Figure 12)

4. For the average curve and upper and lower bounds, multiply the normalized deflection values by the average maximum deflection of the raw curves. (Figure 13)
5. Calculate the average and the S.D. of the deflection at the end point of each raw response curves to obtain a 'box' representing a failure point variation estimated from one standard deviation of the force and deflection. (Figure 14)

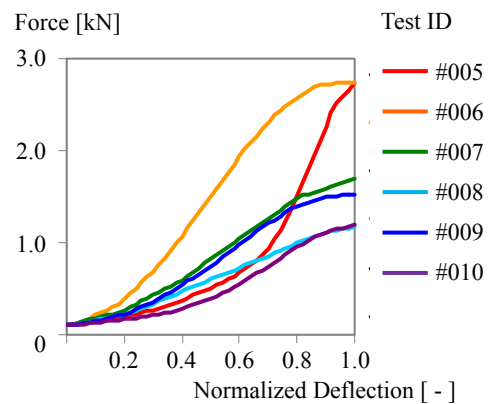


Figure 10. Step 1: Force-Normalized Deflection Responses.

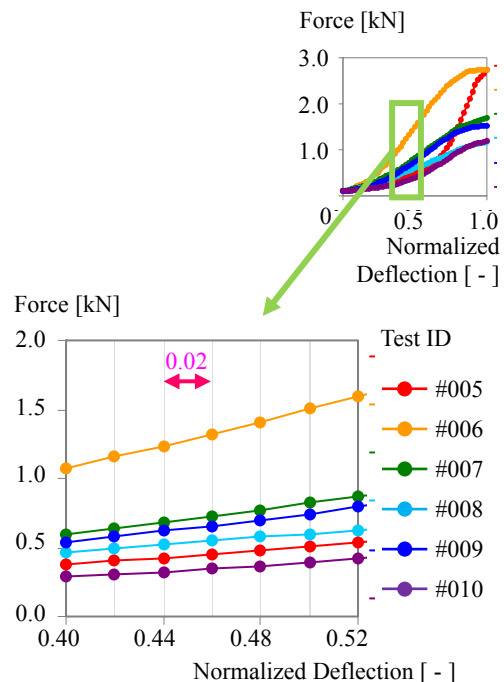


Figure 11. Step 2: Interpolation of Deflection for Force-Normalized Deflection Responses.

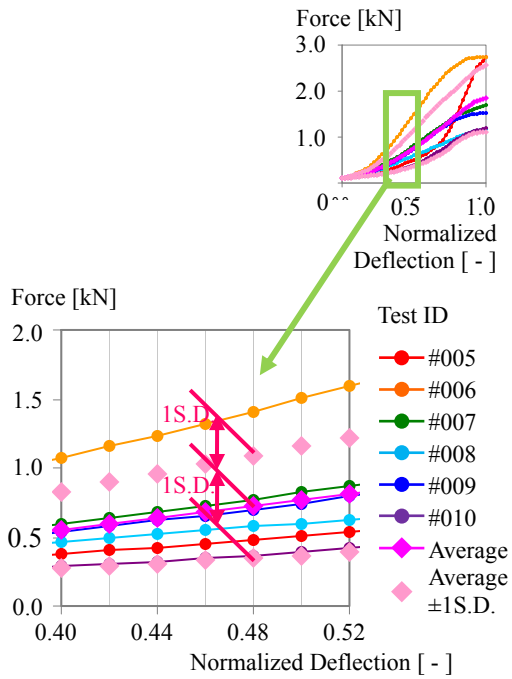


Figure 12. Step 3: Average and Upper and Lower Bounds of Force-Normalized Deflection Responses.

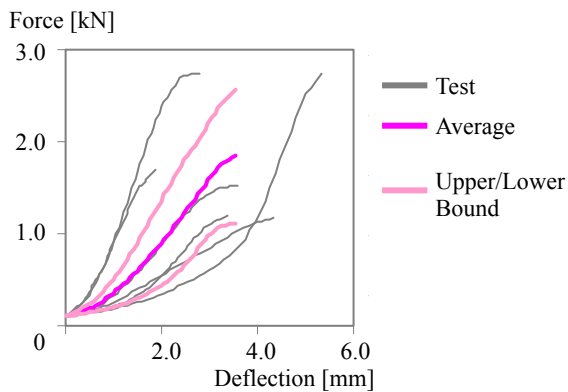


Figure 13. Step 4: Average and Upper and Lower Bounds of Force-Deflection Responses.

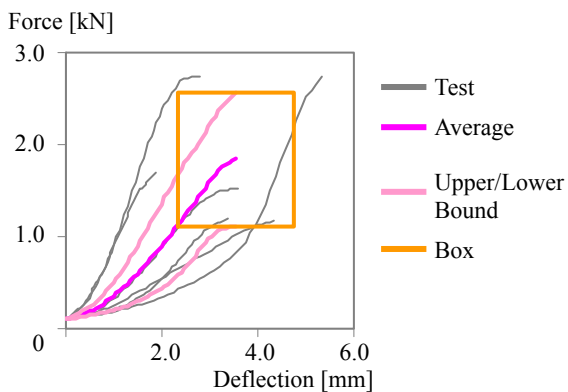


Figure 14. Step 5: 'Box' Representing Failure Point Variation.

MODEL VALIDATION

Pelvis-1: Validation against the experiment by Salzar et al.

Model Setup The modified pelvis model was validated against the dynamic loading tests conducted by Salzar et al. The model setup simulating the experiment is shown in Figure 15.

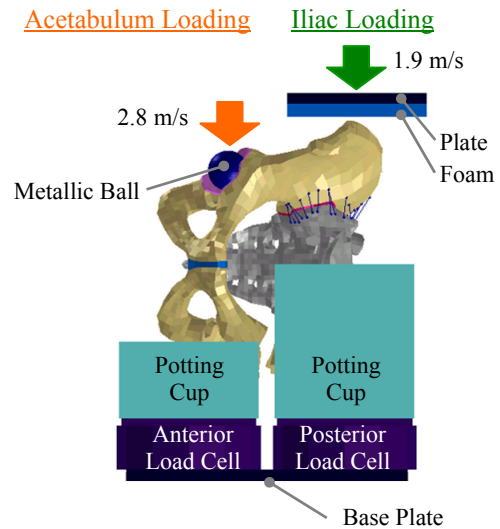


Figure 15. Model Setup Simulating Experiment by Salzar et al. for Pelvis Validation.

Similar to the experimental setup, the translational degree of freedom of the impact surface in anterior-posterior direction and the translational degree of freedom of the base plate to which potting cups are connected via load cells in superior-inferior direction were both set free. As the impact surface, the metallic ball (for acetabulum impact) or the plate (for iliac impact) was modeled as rigid, and the average time history of the displacement of the impact surface calculated from the test results was applied to them. At the surface of the plate, a layer of foam was modeled using solid elements (MAT21). The material property of this foam was determined from dynamic compression tests of CF-45 Confor[®] Foam at the loading rate of 35 km/h and the temperature of 20 °C. On the non-impact side, the elements of the pelvis model along a line defined from the mid distance of the two anterior iliac spines and the top of the greater sciatic notch were removed. The elements within the potting cups on the non-impact side of the pelvis were rigidly connected to the corresponding potting cups modeled as rigid. Each potting cup was connected to the load cell,

which was fixed to the base plate modeled as rigid. Kinematic joint elements were specified at the interfaces between the potting cups and the load cells in order to obtain time histories of the reaction forces.

Results In acetabulum loading, pubic rami fracture was predicted as a result of this simulation (Figure 16). This prediction well matched the results of the experiment, where pubic rami fracture was observed in 5 out of 6 cases. In iliac loading, dislocation of the SI joint was predicted, followed by fracture of the ilium near the SI joint (Figure 17), while SI joint dislocation and bone fracture near the SI joint were observed in 2 and 2 out of 4 cases in the experiment, respectively.

The predicted force-deflection response was compared to the average curve and corridor determined from the results of the experiment (Figures 18 through 21). This comparison showed that the model prediction well matched the average curve for the anterior response in acetabulum loading and the posterior response in iliac loading, which were the major load paths compared to others for both loading configurations.

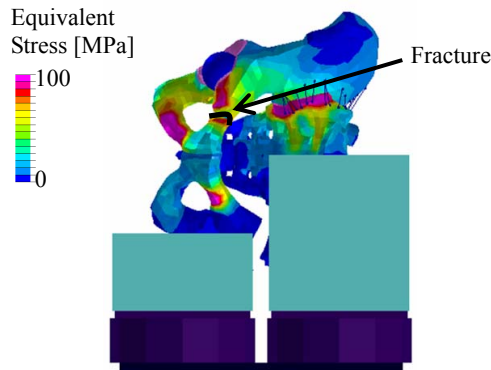


Figure 16. Injury Prediction in Acetabulum Loading.

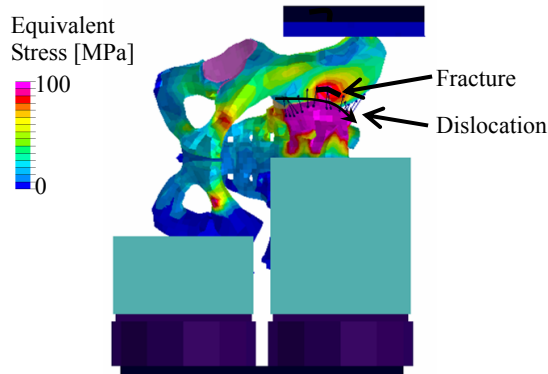


Figure 17. Injury Prediction in Iliac Loading.

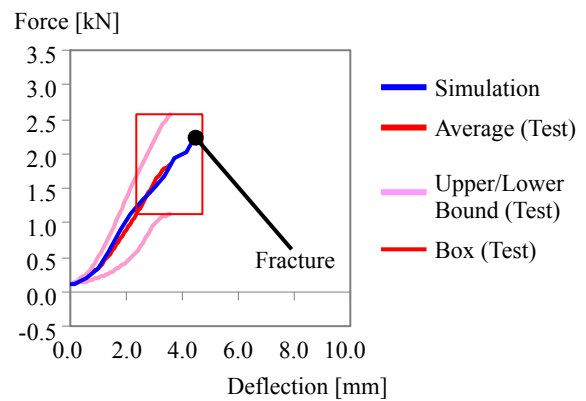


Figure 18. Comparison of Force-Deflection Response for Anterior Reaction Force in Acetabulum Loading.

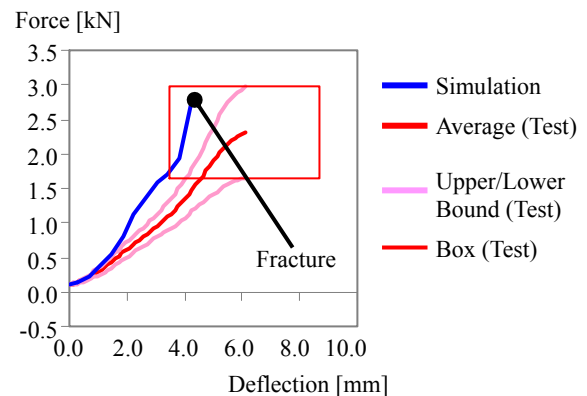


Figure 19. Comparison of Force-Deflection Response for Posterior Reaction Force in Acetabulum Loading.

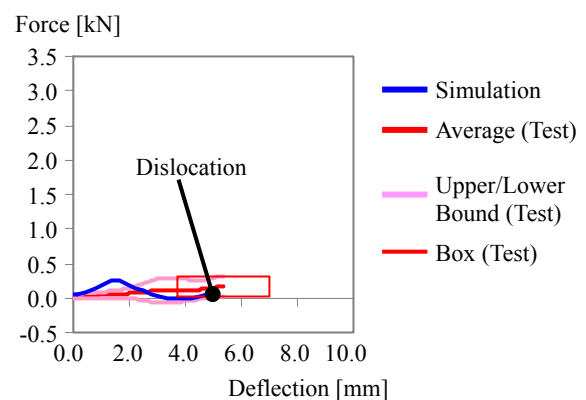


Figure 20. Comparison of Force-Deflection Response for Anterior Reaction Force in Iliac Loading.

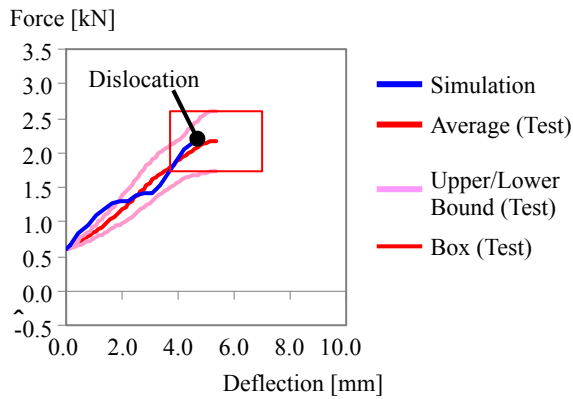


Figure 21. Comparison of Force-Deflection Response for Posterior Reaction Force in Iliac Loading.

Pelvis-2: Validation against the experiment by Guillemot et al.

Model Setup The validation using the results from Guillemot et al. performed in the previous study [Kikuchi et al. 2006] was also done using the modified pelvis model. As shown in Figure 22, one side of the pelvis bone was fixed to the bone fixing box, and a metallic ball inserted into the acetabulum was impacted by the impactor covered with the silicon padding. The material property of the silicon padding was derived from the data used in the previous study. The padding with a dropping mass of 3.68 kg impacted the metallic ball at a speed of 4 m/s.

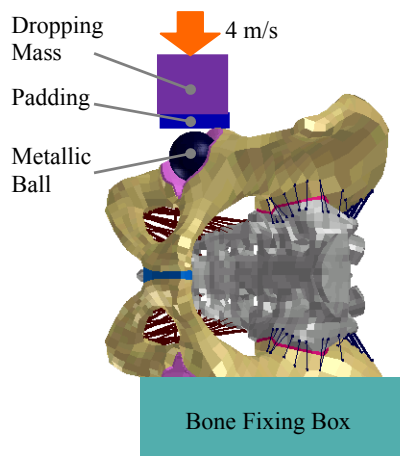


Figure 22. Model Setup Simulating Experiment by Guillemot et al. for Pelvis Validation.

Results The injury prediction from the simulation was shown in Figure 23. Complete fracture of the superior pubic ramus was predicted by the model. The relationship between the maximum force

and the maximum displacement from the results of the test and simulation was shown in Figure 24. Six out of twelve tests were performed using female pelvises. However, since the height of the specimen was not described in the paper, the value of the tests was unable to be scaled to a mid-sized male. The test results are classified into 3 groups depending on injury patterns, and the simulation results fell within the variation range of the maximum force and the maximum displacement for the group sustaining pubic fracture, which was predicted by the model.

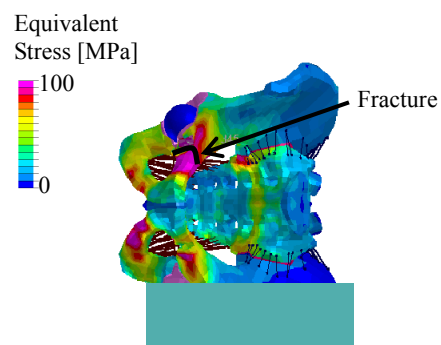


Figure 23. Injury Prediction in Pelvis Validation against Guillemot et al.

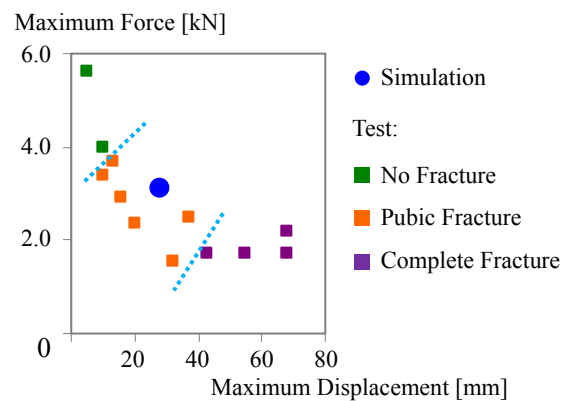


Figure 24. Comparison of Relationship between Maximum Force and Maximum Displacement.

Pubic Symphysis

Model Setup The pubic symphysis model was validated against the compressive loading tests conducted by Dakin et al. [2001] for the compression up to 8 mm. The model setup representing the experiment is shown in Figure 25. The pubic symphysis model along with bony parts on both sides of the pubic symphysis was extracted from the modified pelvis model, and both edges of the pubis were rigidly fixed to the bone fixing boxes. In the simulation, one side of the bone fixing box was fixed

to the space, and enforced displacement in compression at the speed of 1 mm/s was applied to the other side.



Figure 25. Model Setup Simulating Experiment by Dakin et al. for Pubic Symphysis Validation.

Results The comparison of force-deflection response between the test and the simulation is shown in Figure 26. The model response showed good correlation with that of the test.

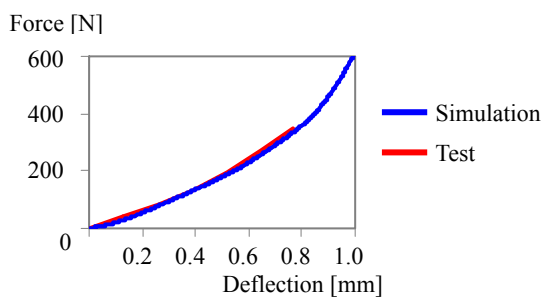


Figure 26. Comparison of Force-Deflection Response of Pubic Symphysis in Compression.

DISCUSSION

The baseline pelvis model developed in a previous study by Kikuchi et al. [2006] incorporated a relatively wider pubic symphysis than that of an actual human. In addition, the model lacked cartilaginous layer at the SI joint. In contrast, the modified model developed in the current study incorporated the pubic symphysis with its geometry taken from CT images, and a layer of cartilage was added at the SI joint. Figures 27 through 30 compare force-deflection responses for the anterior and posterior reaction forces in acetabulum and iliac impacts, respectively, obtained from pelvis lateral loading simulations representing the experiment by Salzar et al. using the pelvis models from the previous study (baseline model) and the current study (modified model). The results of the comparisons showed that the baseline model failed to accurately represent responses on both the anterior and posterior

sides in terms of stiffness and failure characteristics, while the responses from the modified model matched those from the experiment on both the anterior and posterior sides. The mechanical characteristics of the pelvis are determined by a combination of those from the cartilaginous layer and the bony structure in series on both anterior and posterior sides. For this reason, it can be concluded that it was necessary to improve geometric and material characteristics of the cartilaginous layers at the pubic symphysis, acetabulum and SI joint to accurately represent force-deflection responses on both the anterior and posterior sides in a certain impact configuration. This suggests that it is crucial for a human pelvis model to incorporate accurate geometric and material properties of cartilaginous layers along with bony structures in order to accurately reproduce pelvis injuries in car-pedestrian collisions.

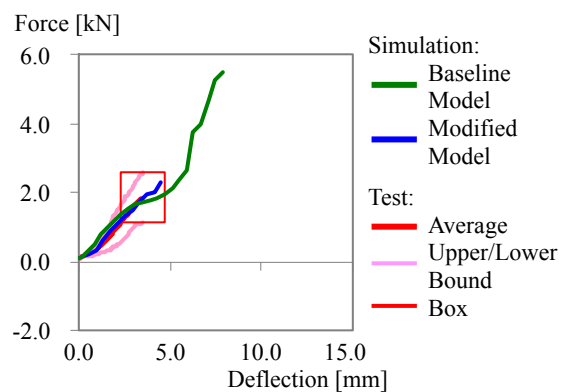


Figure 27. Comparison of Force-Deflection Response for Anterior Reaction Force in Acetabulum Loading between Baseline and Modified Pelvis Models.

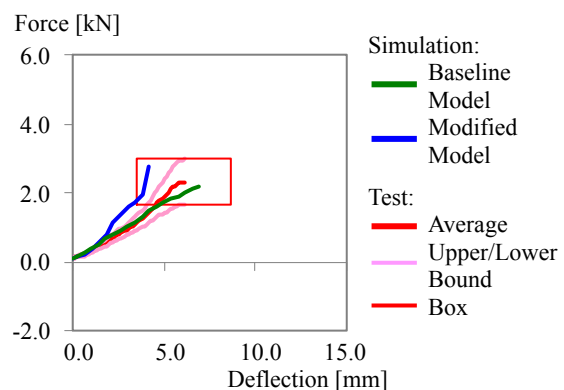


Figure 28. Comparison of Force-Deflection Response for Posterior Reaction Force in Acetabulum Loading between Baseline and Modified Pelvis Models.

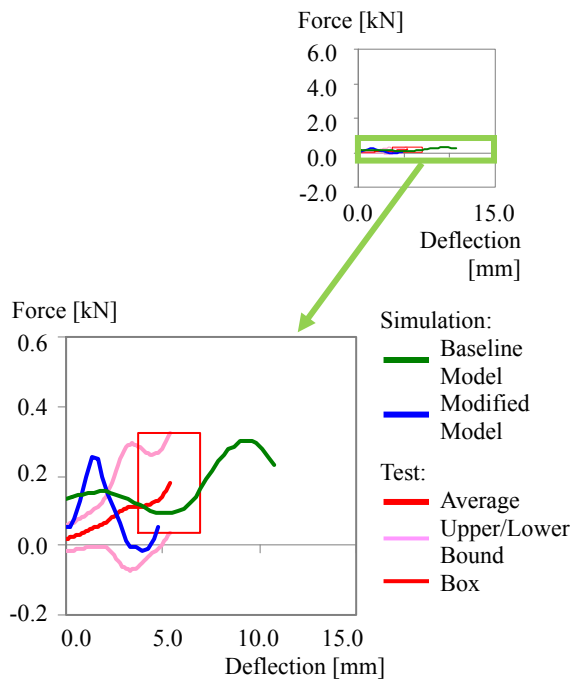


Figure 29. Comparison of Force-Deflection Response for Anterior Reaction Force in Iliac Loading between Baseline and Modified Pelvis Models.

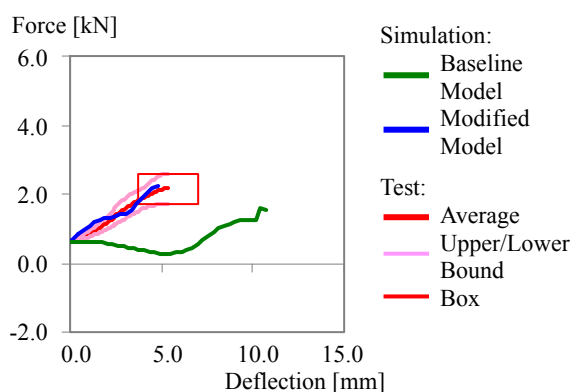


Figure 30. Comparison of Force-Deflection Response for Posterior Reaction Force in Iliac Loading between Baseline and Modified Pelvis Models.

Although the current study extensively validated the modified pelvis model against human response data available from the literature, the model still has some limitations in model validation.

1. The material property of the cartilage of the acetabulum and the SI joint were estimated through the validations, rather than using biomechanical data at the tissue level, because of the lack of data available from the literature. The material parameters for the cartilage used in the modified model need to be further validated once

such data becomes available in the future.

2. The sacrum was modeled as a ductile structure with shell elements representing only the cortical layer, and no trabecular bone inside the sacrum was modeled, due to geometrical complexity. Although the biomechanical data used in the model validations do not include fracture to the sacrum, this would be an issue when predicting sacral fracture and requires further improvement as necessary.
3. The pelvis model was validated primarily in lateromedial direction. Accident statistics in Japan shows that in the year 2009, 59.9% of pedestrian accidents occurred when a pedestrian was walking across the road, and 16.5% of them occurred when a pedestrian was walking toward or parallel to the vehicle. Although the accident data suggest that primary loading direction to a pedestrian pelvis would be in lateral direction, the model needs to be further validated in other directions as well, in order to allow application of the model to prediction of injuries in various real-world situations.

CONCLUSION

In this study, the finite element model for the pedestrian pelvis developed in a previous study was modified by adding layers of cartilage at the acetabulum and the SI joint, and improving the geometry of the pubic symphysis and the orientation of the SI ligaments using the CT images.

The biofidelity of the modified pelvis model was evaluated by performing additional validations against published data, including individual validation of reaction forces at the anterior and posterior sides in acetabulum and iliac impacts.

The results of this study provide a tool for accurate prediction of the load distribution inside the pelvis when the pelvis is subjected to lateral impact.

ACKNOWLEDGEMENTS

The authors would like to thank Nobuhiro Tsukamoto, M.D., of Saitama Medical University for his technical support in collecting CT images.

REFERENCES

- [1] Carter, D.R. and Hayes, W.C. 1977. "The Compressive Behavior of Bone as A Two-Phase Porous Structure" *The Journal of Bone and Joint Surgery*, 59(7): 954-962
- [2] Dakin, G.J., Arbelaez, R.A., Molz, F.J., Alonso, J.E., Mann, K.A. and Eberhardt, A.W. 2001. "Elastic and Viscoelastic Properties of the Human Pubic Symphysis Joint: Effects of Laterla Impact Joint Loading" *Journal of Biomechanical Engineering*, 123(3): 218-226
- [3] Dalstra, M., Huiskes, R. and van Erning, L. 1995. "Development and Validation of a Three Dimensional Finite Element Model of the Pelvis Bone" *Journal of Biomechanical Engineering*, 117: 272-278
- [4] Edwards, K.J. and Green, J.F. 1999. "Analysis of the Inter-Relationship of Pedestrian Leg and Pelvis Injuries" *Proceeding of 1999 International IRCOBI Conference on the Biomechanics of Impacts*, 355-369
- [5] Gray, H. 1995. "Gray's Anatomy: The Anatomical Basis of Medicine and Surgery, Thirty-eighth Edition" Churchill Livingstone
- [6] Guillemot, H., Got, C., Resnault, B., Lavaaste, F., Robin, S., Le Coz, J. and Lassau, J. 1998. "Pelvis Behavior in Side Collisions; Static and Dynamic Tests on Isolated Pelvic Bones" *Proceedings of the 16th International Technical Conference of the Enhanced Safety of Vehicles*, 1412-1424
- [7] Institute for Traffic Accident Research and Data Analysis 2009. "Traffic Accident Statistics" (in Japanese)
- [8] Kemper, A.R., McNally, C. and Duma, S.M. 2008. "Dynamic Tensile Material Properties of Human Pelvic Cortical Bone" *Biomedical Science Instrumentation*, 44:417-418
- [9] Kikuchi, Y., Takahashi, Y. and Mori, F. 2006. "Development of a Finite Element Model for a Pedestrian Pelvis and Lower Limb" *SAE Paper #2006-01-0683*
- [10] Kikuchi, Y., Takahashi, Y. and Mori, F. 2008. "Full-Scale Validation of a Human FE Model for the Pelvis and Lower Limb of a Pedestrian" *SAE Technical Paper #2008-01-1243*
- [11] Konosu, A. 2003. "Development of a Biofidelic Human Pelvis FE-Model with Several Modifications onto a Commercial Use Model for Lateral Loading Conditions" *SAE paper #2003-01-0163*
- [12] Lessley, D., Crandall, J., Shaw, G., Kent and R., Funk, J. 2004. "A Normalized Technique for Developing Corridors from Individual Subject Responses" *SAE Technical Paper #2004-01-0288*
- [13] McElhany, J.M., Roberts, V.L. and Hilyard, J.F. 1976. "HANDBOOK OF HUMAN TOLERANCE" Japan Automobile Research Institute, Inc.
- [14] McLauchlan, G.J. and Gardner, D.L. 2002. "Sacral and Iliac Articular Cartilage Thickness and Cellularity; Relationship to Subchondral Bone End-Plate Thickness and Cancellous Bone Density" *Rheumatology*, 41(4): 375-380
- [15] Ostertag, A., Cohen-Solal, M., Audran, M., Legrand, E., Marty, C., Chappard, D. and de Vernejoul, M. 2009. "Vertebral Fractures are Associated with Increased Cortical Porosity in Iliac Crest Bone Biopsy of Men with Idiopathic Osteoporosis" *Bone*, 44: 413-417
- [16] Plummer, J.W., Bidez, M.W. and Alonso, J. 1996. "Parametric Finite Element Studies of the Human Pelvis: The Influence of Load Magnitude and Duration on Pelvis Tolerance During Side Impact" *SAE Technical paper #962411*
- [17] Renaudin, F., Guillemot, H., Lavaste, F., Skalli, W., Lesage, F. and Pecheux, C. 1993. "A 3D Finite Element Model of Pelvis in Side Impact" *SAE Technical Paper #933130*
- [18] Robbins, D.H. 1983. "Anthropometric Specifications for Mid-sized Male Dummy, Volume 2, the University of Michigan Transportation Research Institute" Report Number UMTRI-83-53-2
- [19] Ryan, P. 1971. "Traffic Injuries of the Pelvis at ST.Vincent's Hospital, Melbourne" *The Medical Journal of Australia*, 1(9): 475-479.
- [20] Salzar, R.S., Genovese, D., Bass, C.R., Bolton, R., Guillemot, H., Damon, A.M. and Crandall, J.R. 2008. "Load Path Distribution within the Pelvic

Structure under Lateral Loading" International Crashworthiness Conference, 14(1): 99-110

[21] Song, E., Trosseille, X. and Guillemot H. 2006. "Side Impact: Influence of Impact Conditions and Bone Mechanical Properties on Pelvic Response Using a Fracturable Pelvis Model" SAE Technical Paper #2006-22-0004

[22] Teresinski, R. and Madro, R. 2001. "Pelvis and Hip Joint Injuries as a Reconstructive Factors in Car-to-Pedestrian Accidents" Forensic Science International, 124: 68-73

[23] Untaroiu, C.D., Salzar, R.S., Guillemot, H. and Crandall, J.R. 2008. "The Strain Distribution and Force Transmission Path Through Pubic Rami During Lateral Pelvic Impacts" International Mechanical Engineering Congress and Exposition, IMECE2008-67791, 79-88

[24] Vix, V.A. and Ryu, C.Y. 1971. "The Adult Symphysis Pubis: Normal and Abnormal" American Journal of Roentgenology, Radium Therapy, and Nuclear Medicine, 112(3): 517-525

[25] Walker, J.M. 1992. "The Sacroiliac Joint: A Critical Review" Physical Therapy, 72(12): 903-916